Unoccupied electronic states in Au(100) surfaces

1994 J. Phys.: Condens. Matter 6 7227

(http://iopscience.iop.org/0953-8984/6/36/007)

J. Phys.: Condens. Matter 6 (1994) 7227–7237. Printed in the UK

Unoccupied electronic states in Au(100) surfaces

F Ciccacci†, S De Rossi†, A Taglia† and S Crampin‡

† Dipartimento di Fisica, Politecnico di Milano, Piazza Leonardo da Vinci 32, I-20133 Milano, Italy

‡ Cavendish Laboratory, Madingley Road, Cambridge CB3 0HE, UK

Received 19 May 1994, in final form 13 June 1994

Abstract. We present a joint experimental and theoretical work on the empty states of Au(100) surfaces. Both the stable 5×10 reconstructed and the metastable defect-stabilized 1×1 surfaces have been investigated by means of angle-resolved inverse photoemission, and the electronic structure has been theoretically determined for the 1×1 surface within the local density approximation. The experimental spectra for the two surfaces are very similar, showing in both cases bulk derived transitions and a surface feature corresponding to the $n = 1$ image-potential state. In the spectra from the metastable surface, a strong $n = 0$ surface resonance is also observed. Comparison with theoretical calculations for the 1×1 surface gives generally good agreement for the bulk transitions, but suggests that surface defects strongly influence surface states localized near the surface layer.

1. Introduction

The electronic structure of noble metal surfaces has been studied in great detail by a variety of electron spectroscopies, deriving information about bulk and surface states. Particularly interesting in this field are angle-resolved spectroscopies, probing electron energies E as well as corresponding momenta $\hbar k$. The most important experimental technique for investigating the occupied states is the well known photoemission spectroscopy [1, 2]. Its counterpart for the empty states, inverse photoemission (IPE) spectroscopy, is an ideal tool for studying the electronic states above the Fermi level [3, 4]. In this spectroscopy, an electron beam impinges on the sample surface and the photons emitted following the radiative transition to empty states are detected. If the electron beam is collimated, as in angle-resolved experiments, the corresponding k-resolved spectroscopy (KRIPE) can be used to perform empty states band mapping, i.e. to picture the dispersion relation $E(k)$ for the empty states, provided that the photon momentum is negligible with respect to the electron momentum, as is the case in the ultraviolet range. Then the IPE spectrum corresponds to radiative direct transitions, i.e., transitions which are essentially vertical in a reduced Brillouin Zone (BZ) scheme. Despite the short penetration depth of low-energy electrons [5], the spectra are often dominated by bulk derived transitions, but emission associated with surface states is also observed. A characteristic feature in the IPE spectra is the presence of peaks associated to image states, which are a direct consequence of the image coulombic potential felt by the electron outside the metal surface. Theory predicts a complete Rydberg series of surface states (each labeled with a quantum number $n = 1, 2, \ldots$) converging towards the vacuum level [6, 3, 4], whereas IPE experiments in general show only the $n = 1$ state, due to instrumental resolution limits [7, 8]. Moreover, other surface states or resonances can be detected [9], which are a consequence of the crystal potential itself and are much

0953-8984/94/367227+11$19.50

more confined at the surface: these states can also be formally classified together with the previous ones as $n = 0$ states [6].

IPE measurements on noble metal surfaces have been performed by various authors and a large database is presently available (see for instance [4] and [10] and references therein for IPE data on the low-index surfaces of Cu and Ag, respectively). Moreover, a very accurate IPE study at normal incidence on the bulk and surface electronic structure of the (100) surfaces of Cu, Au, Ag, and Cu_3Au has been recently performed [11], in view of their importance as substrates for a variety of promising magnetic films. Reference [11] also contains a quite complete set of references to previous investigations, which the reader is referred to.

Despite these extensive works, however, a systematic study of the empty energy bands in Au(100) with KRIPE is still missing. This fact represents a considerable limitation, since the knowledge of the clean surface electronic structure is a prerequisite for studying the properties of interesting overlayers deposited onto it. For instance, Fe thin films grown on Au(100) exhibit enhanced magnetic moments according to theoretical predictions [12, 13], and several experimental results have been reported confirming the relevance of such systems [14].

Moreover, the clean Au(100) surface, at variance with most of the other noble metal surfaces, exhibits a reordered atomic structure leading to the 5×20 reconstruction, which results from a close-packed hexagonal surface layer superimposed to the square net of the (100) surface [15]. On the other hand, the 'normal' 1×1 surface can be obtained as a metastable structure stabilized by impurities or defects [16, 17]. This complex structure may be useful in order to disentangle surface related features from bulk-like transitions usually predominant in the spectra.

The aim of the present work is to investigate empty electronic states in Au(100) in detail. In particular, we report on angle-resolved data along the ΓXUL and ΓXWK symmetry planes of the FCC BZ, for both the 1×1 and 5×20 reconstructed surfaces. Theoretical calculations determining the electronic structure of the Au(100)-1×1 surface are also presented and compared with experiments.

2. Experimental procedure

The experimental set-up has been described in detail elsewhere [18]. Briefly, it consists of a ultra-high vacuum (UHV, pressure in the low 10^{-10} Torr range) system, equipped with several surface characterization and sample preparation techniques, and containing an IPE apparatus.

Spectra are taken in the isochromat mode, collecting the emitted photons at a fixed energy while changing the electron beam energy. A low-energy electron gun, based on photoemission from a negative electron affinity GaAs photocathode, produces a transversely beam (beam polarization is not used in the present experiment) [19]. Light emitted from the sample following a radiative transition is detected by a high-efficiency band-pass photon detector, based on the combined filtering action of a KBr photocathode and a UV window [20]. In the present experiment the detector energy resolution has been improved with respect to that previously reported by using SrF_2 instead of CaF_2 as entrance window material. This changes the short-wavelength transmission limit from 1220 Å (about 10.2 eV) to 1280 Å (9.7 eV) [21]. As a consequence, the centre band-pass energy shifts from 9.8 to 9.6 eV and, more importantly, the energy resolution (full width at half maximum, FWHM) is improved from ± 0.5 eV to about ± 0.3 eV. The effect of the better resolution is shown

in figure 1, where we have reported IPE spectra taken on the same Ag(100) surface with the two different windows under otherwise identical conditions. The total instrumental resolution can be obtained from the width of the $n = 1$ image state at 3.9 eV above the Fermi level E_F. In fact, it is well known that this feature is very sharp and the width is essentially determined by the experimental resolution [22]. The most accurate estimate of the intrinsic width of the image-potential state is 0.1 eV, as obtained by the measured value of 0.25–0.3 eV with the best experimental resolution reported so far [8, 11]. As shown in figure 1, with the new set-up the width of the peak, which also includes the 0.25 eV electron source contribution [19], is 0.7 eV at FWHM. Since the natural width is very small, this value represents an upper limit for the overall instrumental resolution of our IPE apparatus.

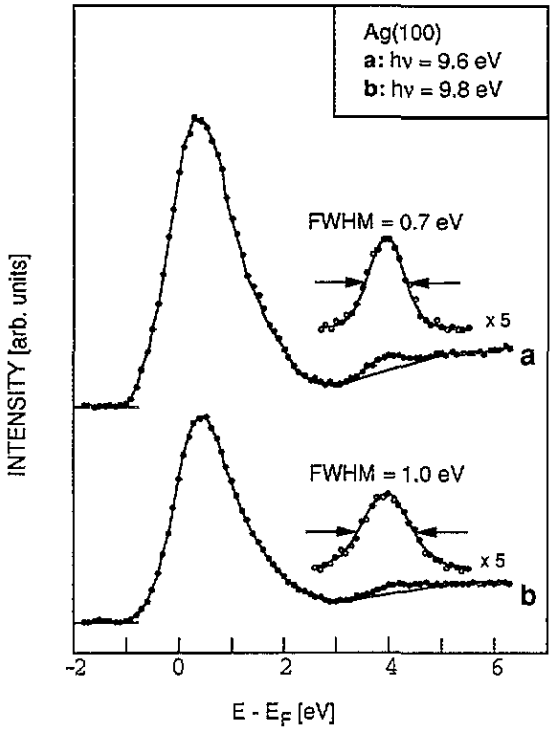

Figure 1. Inverse photoemission spectra from Ag(100) at normal incidence. Data have been taken using a CaF_2 (a) or a SrF_2 (b) entrance window in the band-pass photon detector. For a better comparison, the contributions from the image-potential surface state at 3.9 eV above E_F are enlarged by a factor 5 after a linear background subtraction.

Clean and well ordered surfaces were obtained by the well known procedure based on 0.5–1 keV Ar in sputtering followed by 500 ° annealing. After some cycles of such treatment the surface did not present any trace of contaminants as seen by x-ray photoemission spectroscopy (XPS) and exhibited a very sharp 5×20 low-energy electron diffraction (LEED) pattern. Such surfaces were very stable, with no change even after several hours of IPE spectra acquisition.

It has been reported that an unreconstructed 1×1 Au(100) surface can be prepared by reactive ion bombardment [16, 17], and more recently a similar structure has also been obtained by normal sputtering not followed by annealing [11]. Our investigation

indicates that surfaces with a sharp 1×1 LEED pattern can be obtained by prolonged Ar ion bombardment. We find that, operating a differentially pumped Ar gun at 1 keV and sample current density of 3 μA cm^{-2}, it takes almost one hour to convert the surface from the 5×20 to the 1×1 reconstruction. Such a procedure produces a metastable structure which rapidly converts back to the stable 5×20 configuration upon heating at about 100 °C. Also for these surfaces XPS analysis did not show any impurity peak, suggesting that the metastable structure is stabilized by defects.

3. IPE results

3.1. 5 × 20 reconstruction

The *k*-resolved measurements have been carried out by rotating the sample around the [010] and [011] directions of the Au lattice. This corresponds to selecting the electron wavevector in the ΓXWK and ΓXUL symmetry planes of the FCC BZ, respectively. When the electron crosses the surface, the parallel component $k_{\parallel}$ of the wavevector is conserved, apart from a generally vanishing [4] surface reciprocal lattice vector.

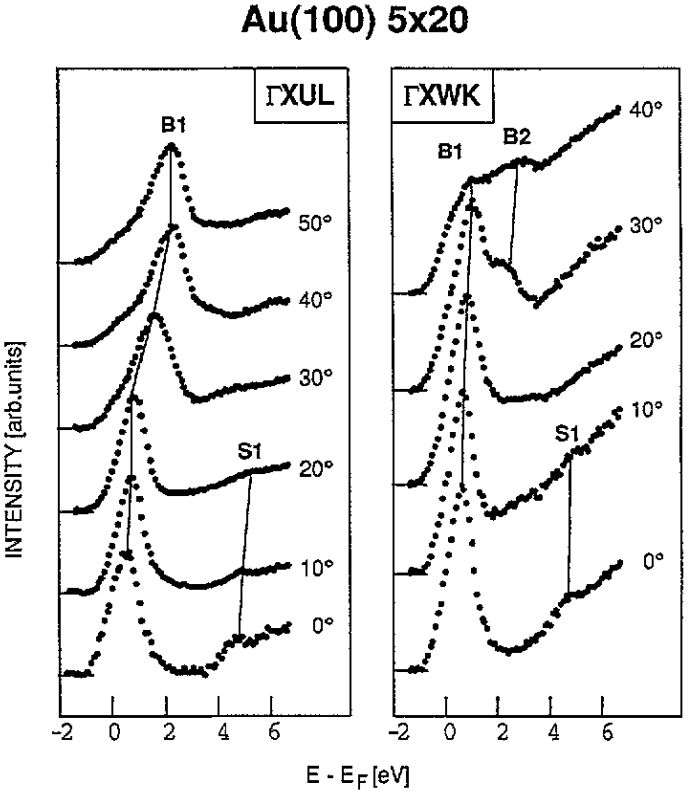

Figure 2. *k*-resolved inverse photoemission spectra at $h\nu = 9.6$ eV from the 5×20 reconstructed Au(100) surface for various electron incidence angles in the ΓXWK and ΓXUL azimuths of the bulk FCC BZ. The spectra have been normalized to equal maximum amplitude. The lines are drawn as a guide for the eye.

We present first the results for the 5×20 reconstructed surface. Typical isochromat spectra for electrons incident at various polar angles in the two planes are shown in figure 2. At $\theta = 0°$ a large peak B1 slightly above E_F and a smaller feature S1 at about 4.7 eV are clearly visible. By inspection of the Au bulk band structure [23] (see also the discussion in section 4 below), we find that B1 can be attributed to bulk transitions. In fact, at normal incidence, corresponding to an electron wavevector along the ΓX line of the bulk BZ, a transition at $h\nu = 9.6$ eV occurs near X from the lower branch of the pair resulting from spin-orbit splitting of a Δ_5 band to a Δ_1 band (both bands have Δ_6 symmetry in the double-group notation).

On the other hand, the second structure S1, which falls in an energy forbidden region, does not correspond to any bulk-like transition and is ascribed to radiative decay into the $n = 1$ image-potential surface state. These identifications agree with normal incidence studies already published [8, 11].

For off-normal incidence in the ΓXUL azimuth, B1 remains the most prominent peak in the spectra, while S1 disappears for incidence angles larger than 20°. Both features disperse towards higher energies; the dispersion of B1 is quite large (almost 2 eV) as compared to the small energy variation of S1. In the ΓXWK azimuth a similar behaviour is seen, though with a less pronounced dispersion of B1. Moreover, in this case, for angles greater than 25° another peak, B2, appears and eventually dominates in the spectra at large incidence angles.

The $E(k_\parallel)$ curve for the image-potential surface state presents a parabolic behaviour, corresponding to a kinetic energy term $(\hbar k_\parallel)^2/2m^*$ to be added to the energy of the state at $k_\parallel = 0$, where the effective mass m^* accounts for the deviation from a simple free-electron behaviour [3, 4]. The fit of our data yields $m^* = (1.5 \pm 0.3)\ m_e$, a value well within those reported for other noble metal surfaces [8, 24].

3.2. 1×1 *reconstruction*

A direct comparison between normal incidence spectra taken from the reconstructed and unreconstructed surfaces is shown in figure 3. The major difference is the presence in the spectrum from the 1×1 surface of a double-structured peak in the first 2 eV above E_F. This structure can be considered as originating from two contributions as shown in the figure. The first contribution just above E_F corresponds well with the B1 peak of the 5×20 surface and can be identified in the same way as derived from a bulk transition. The second one, labeled S0, is new however, being completely absent in the 5×20 case. Moreover, the fact that it has no counterpart in the bulk derived transitions points towards its identification as a surface-related structure. On other noble metal surfaces [9, 11] a corresponding feature has been ascribed to a $n = 0$ surface resonance. Note that in this case the resonance is very pronounced being predominant in the spectrum, at variance with the findings on Ag and Cu [4, 6, 10]. A similar $n = 0$ peak is instead absent in the Au(100) 5×20 surface, probably due to the different surface structure, as already suggested [11].

Considering next the $n = 1$ image-potential state, we see this feature is present in both surfaces. In the 1×1 surface, however, the $n = 1$ state is found at slightly higher energies, about 4.8 eV above E_F [25]. Moreover, the peak is less intense as compared to the case of the 5×20 reconstruction. This result could be expected by considering how sensitive the image state peaks are to the quality and flatness of the surface [4, 11]. Obviously, the metastable 1×1 surface which is stabilized by defects, cannot be considered to be very ordered. The width of the peak, however, remains unchanged (0.7 eV at FWHM). As noted above, this is mainly due to experimental resolution limits.

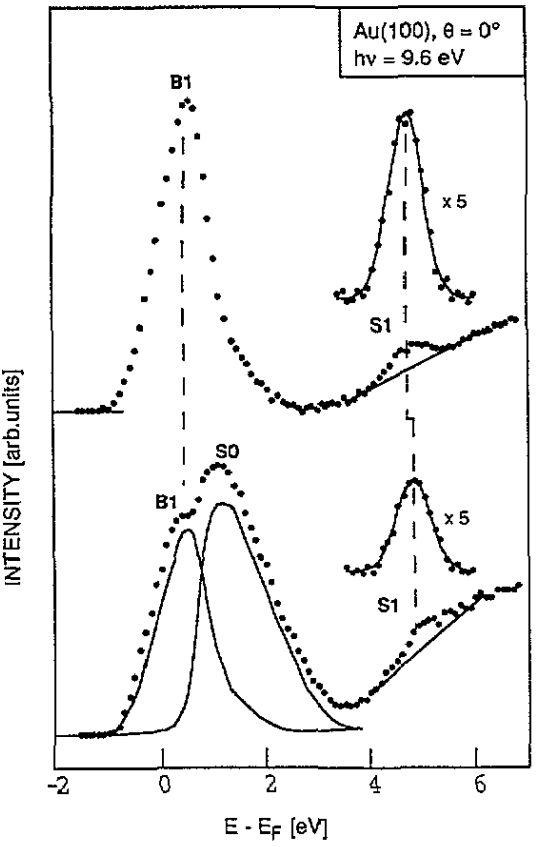

Figure 3. Normal incidence inverse photoemission spectra from the 5 × 20 and the metastable 1 × 1 Au(100) surfaces (upper and lower curves, respectively). Decomposition of the peak just above E_F in the 1 × 1 case is presented as full lines. The peaks S1 are shown also enlarged by a factor 5 after a linear background subtraction. The dashed lines are drawn as a guide for the eye.

The picture which arises from the comparison of the $\theta = 0°$ spectra discussed above, i.e., a very similar behaviour but with an extra structure in the 1 × 1 with respect to the 5 × 20 spectrum, is confirmed by the off-normal data. Figure 4 shows a set of isochromat spectra taken from the metastable 1 × 1 surface at different incidence angles in the ΓXUL and ΓXWK azimuths, corresponding to the $\bar{\Gamma}\bar{X}$ and $\bar{\Gamma}\bar{M}$ directions of the square surface BZ respectively. It is seen that B1 and S1 disperse towards higher energies in the same way as in the 5 × 20 surface, while the new structure S0 does not present any appreciable energy variation. In both azimuths for incidence angles larger than 20°, S1 is no longer visible, while B1 and S0 merge together. A new structure B2 appears at angles larger than 25° in the ΓXWK azimuth, again in the same way as in the 5 × 20 surface.

4. Comparison with theoretical calculations

The experimental results for the two surfaces are summarized in figure 5 (upper and lower panels for the 5 × 20 and 1 × 1 surface, respectively), where we shown an $E_f(k_\parallel)$ energy

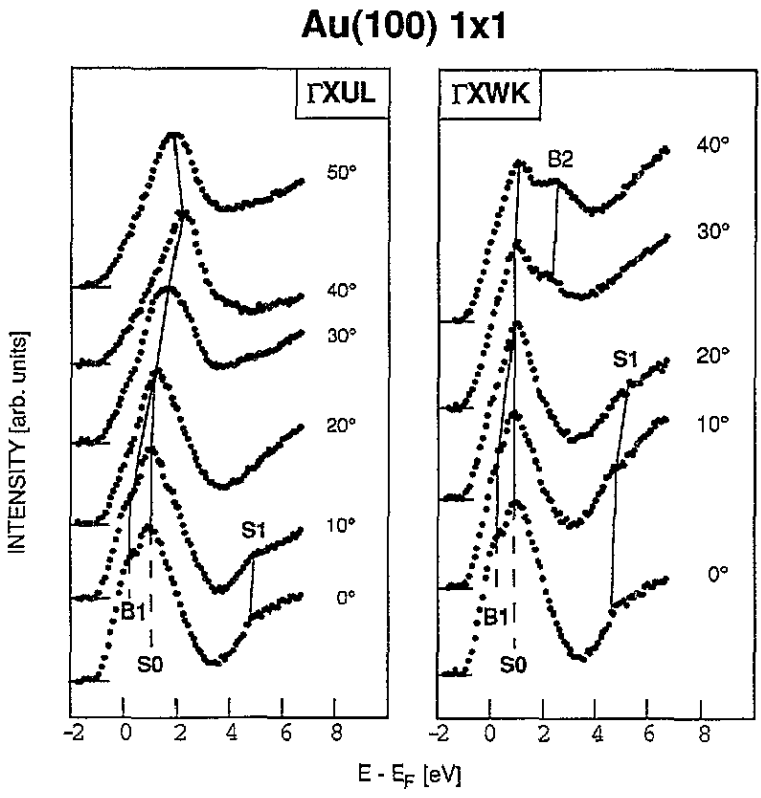

Figure 4. *k*-resolved inverse photoemission spectra at $h\nu = 9.6$ eV from the metastable 1×1 Au(100) surface for various electron incidence angles in the ΓXWK and ΓXUL azimuths of the bulk FCC BZ. The spectra have been normalized to equal maximum amplitude. The lines are drawn as a guide for the eye.

diagram, i.e., the final energies of the transitions as a function of the parallel component of the wavevector. As noted above, the results for the 1×1 surface are identical to the ones for the 5×20 surface, apart from the flat band near the centre of the surface BZ, corresponding to the surface resonance S0. The other surface-related structure, i.e., the $n = 1$ image-potential state presents the same dispersion in both surfaces within experimental errors, so that the estimated effective masses turn out to be the same, $m^*/m_e = 1.5 \pm 0.3$.

To further understand these results we have determined the electronic structure of the Au(100)-1×1 surface theoretically, in the local density approximation (LDA). For this we have employed the layer KKR method with the atomic sphere approximation, as previously used for the Fe/Au study in [13], where technical details may be found. For the current study the partial wave expansions have been increased to include all states with angular momentum up to and including $l = 4$, which has recently been shown to give an improved description of the electron density at the solid–vacuum interface [26]. Both substrate and surface have been recalculated self-consistently with this larger basis. For the bulk, the main difference with the results of [13], and already anticipated there, is to place the Fermi level lower down relative to the electron states, so that the X_4, level is now at +1.4 eV. These calculations are scalar-relativistic, which ignores spin-orbit coupling.

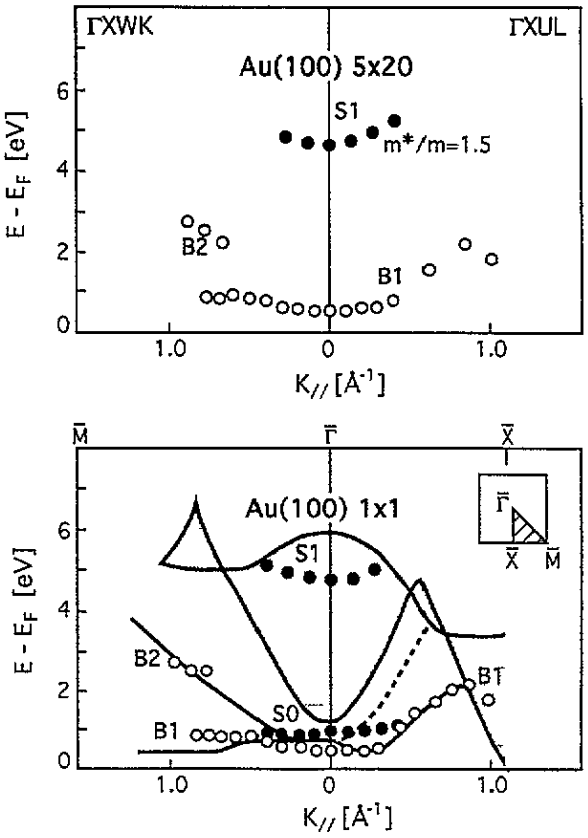

Figure 5. Empty band dispersion versus the parallel component of the electron wave vector in the ΓXWK and ΓXUL bulk mirror planes for the 5×20 (top panel) and the 1×1 (lower panel) surfaces. Full and empty dots refer to surface and bulk derived transitions respectively. For the 1×1 case, the band gaps of the bulk projected structure are also shown as shaded areas. The lines are the theoretical curves as obtained from the calculated bulk band structure: full and dashed lines refer to transitions respectively allowed and forbidden by symmetry (see text).

4.1. Bulk bands

The comparison between the spectra relative to the two reconstructions indicates very similar behaviour of the empty states in the two surfaces. In particular, both surfaces give rise to similar bulk-related transitions. This is not obvious since in the 5×20 case, because of the reduced surface periodicity, folding of the bulk bands occurs, leading to a much smaller surface BZ. Therefore emission of extra peaks from the bulk due to surface umklapp processes introduced by the hexagonal surface layer could be expected. Such contributions, however, may usually be neglected in clean metal surfaces [17], indicating that diffraction by the topmost layer is quite weak so that the electron sees mostly the 1×1 bulk unit cell. Therefore the following discussion applies to the 5×20 surface as well.

The bulk band structure $E(k_z, k_\parallel)$ has been evaluated for $k_\parallel$ along $\bar{\Gamma}\bar{X}$ and $\bar{\Gamma}\bar{M}$ and from this, the projected band structure has been obtained. The band gaps of the projected bulk band structure are shown in the lower panel of figure 5 as shaded areas. We have also determined the bulk transitions which occur at $h\nu = 9.6$ eV for various $k_\parallel$. The final energies of the transitions versus $k_\parallel$ are indicated in the lower panel of figure 5 (full lines),

to be compared with the experimental results (open circles). This comparison for the bulk transitions is quite satisfactory; in particular the dispersion of the peak B1 is very well reproduced. From the band structure other transitions towards states at higher energies are also found, corresponding to the peak B2, which is, however, observed only along $\bar{\Gamma}\bar{M}$ at large incidence angles and is completely absent in the spectra along $\bar{\Gamma}\bar{X}$. The reason for this must be looked for in the symmetry of the bands involved in the transition. In fact, the electron wavefunction must have either even or odd parity under reflection in a mirror plane, in our case the ΓXWK and ΓXUL planes of the FCC BZ for $k_\parallel$ along $\bar{\Gamma}\bar{M}$ and $\bar{\Gamma}\bar{X}$, respectively. The incident electron plane wave, however, has even parity and consequently couples only to bulk states with even parity. Therefore we only have to consider even states as initial ones. Thus matrix elements connect the initial states to final ones with appropriate symmetry. Such symmetry depends upon the polarization of the emitted radiation. Light with electric vector normal to the mirror plane (odd) results from transition to final states of odd parity, while polarization parallel to the mirror plane signals final state functions with even parity. In our measurements we are not sensitive to the light polarization so that both even and odd final states can be reached. From the calculations, we find that the initial state corresponding to transition B2 along $\bar{\Gamma}\bar{X}$ is odd, which explains the absence of this transition in the experimental spectra, whilst B1 along $\bar{\Gamma}\bar{X}$ and B1 and B2 along $\bar{\Gamma}\bar{M}$ have initial states of even symmetry. The reason why B2 is seen only at large angles along $\bar{\Gamma}\bar{M}$ is probably the result of an intensity effect which makes the lower transition much more prominent. Such effects are not included in the symmetry arguments discussed so far. To make this point clear a full calculation of the IPE process, which is beyond the purpose of the present discussion, would be necessary.

4.2. Surface states

By calculating the local density of states at the surface, a number of surface states have also been identified, and the dispersion of these states is indicated in figure 6. Of particular interest is the state labeled S1, which lies at 4.84 eV (0.69 eV below the vacuum level) at $\bar{\Gamma}$ and disperses with effective mass $m^* = 1.2m_e$. This state clearly corresponds to the image state seen in the IPE spectra, confirmation being found by inspection of the calculated charge distribution of the level which shows the maximum of the wavefunction lies well outside the surface. It is remarkable that this state should be found within a calculation which uses the LDA, which omits the coulombic image potential which would give rise to a complete Rydberg series of levels. Clearly the LDA itself generates a vacuum barrier sufficiently deep to bind the level, though not surprisingly no higher levels are found. The effective mass is consistent with the value measured in the IPE experiment, which tends to suggest that the departure from free-electron dispersion is a real effect, probably because in this case the state is not created purely by the image-like part of the surface potential. The state is found to exist over a range of $k_\parallel$ comparable to the experiment, beyond which the state overlaps in energy with the continuum and vanishes almost immediately.

As reported previously [13], a conventional surface state is also located at $\bar{\Gamma}$ within the calculation, although increasing the basis brings it closer to the band edge, only 0.05 eV above. Away from the zone centre the state becomes even closer to the band edge before entering the continuum as a resonance which rapidly broadens and vanishes. This behaviour is at variance with the IPE experiments, which shows the S0 feature degenerate with bulk bands. Furthermore, attempts to improve agreement by introducing a contraction of the surface interlayer spacing are unsuccessful, and by applying shifts to the potential of the surface Au we have established that the surface state is not particularly sensitive to the potential. The origin of the discrepancy is therefore most likely to lie with the atomic

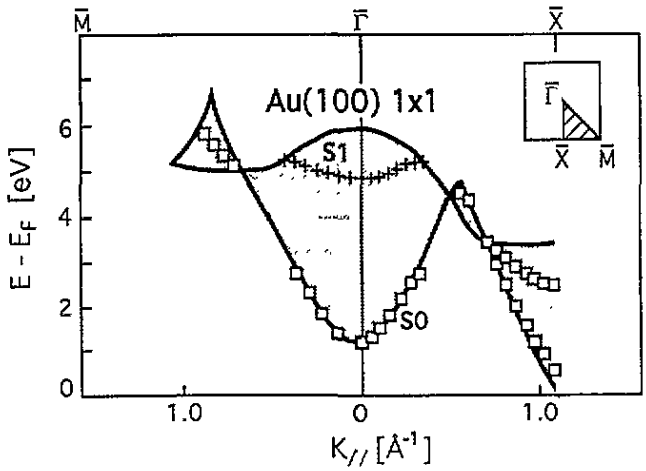

Figure 6. Calculated electronic structure of the Au(100)-1 × 1 surface. The band gaps of the projected bulk band structure are represented by the shaded areas. Surface states dispersion curves are indicated as full lines.

structure of the defect stabilized 1 × 1 surface, which may be sufficiently disrupted to radically alter surface states which are strongly localized near the surface layer. A localized state resulting from surface defects, in fact, would be consistent with the dispersionless S0 feature found in the experiment.

5. Summary

We have presented an angle resolved inverse photoemission study from the (100) surface of gold along the ΓXWK and ΓXUL symmetry planes of the bulk Brillouin zone. In particular, we have studied both the stable surface which presents a 5 × 20 reconstruction and the unreconstructed 1 × 1 surface, which has been obtained as a defect-stabilized metastable surface by prolonged Ar ion sputtering not followed by annealing. Our measurements indicate that as far as the empty states are concerned the two surfaces are quite similar. The spectra are dominated by bulk-derived transitions which are present at the same energy and present the same dispersion with $k_{\parallel}$ in both cases. Moreover a surface feature related to the $n = 1$ image-potential state is present in the spectra from the two surfaces; it is found at slightly different energies (4.7 and 4.8 eV for the 5 × 20 and 1 × 1 surfaces at $k_{\parallel} = 0$) and shows a similar dispersion, yielding the same effective mass $m^*/m_e = 1.5 \pm 0.3$ for both surfaces. The major difference between the two surfaces if the presence of a flat and strong $n = 0$ surface resonance in the 1 × 1 surface, which is absent in the 5 × 20 case.

Theoretical calculations determining the electronic structure of the Au(100)-1 × 1 surface have also been performed. Comparison between theory and experiment give generally good agreement for the bulk transitions, but suggest surface defects strongly influence surface states localized near the surface layer.

Acknowledgments

We would like to thank L Duo' for fruitful discussions. Financial support from the Ministero

dell'Universita' e della Ricerca Scientifica through the Consorzio Istituto Nazionale di Fisica della Materia is also acknowledged.

References

[1] Himpsel F J 1983 *Adv. Phys.* **32** 1
[2] Plummer W E and Eberhardt W 1982 *Adv. Chem. Phys.* **49** 553
[3] Smith N V 1988 *Rep. Prog. Phys.* **51** 1227
[4] Andrews P T, Collins I R and Inglesfield J E 1992 *Unoccupied Electronic States* ed J C Fuggle and J E Inglesfield (Berlin: Springer) p 243
Scneider R and Dose V 1992 *It Unoccupied Electronic Stated* ed J C Fuggle and J E Inglesfield (Berlin: Springer) p 277
[5] Seah M P and Dench W A 1979 *Surf. Interf. Anal.* **1** 2
[6] Echenique P M and Pendry J P 1978 *J. Phys. C: Solid State Phys.* **11** 2065
[7] Dose V, Altmann W, Goldmann A, Kolac U and Rogozik J 1984 *Phys. Rev. Lett.* **52** 1919
[8] Straub D and Himpsel F J 1984 *Phys. Rev. Lett.* **52** 1922; 1986 *Phys. Rev.* B **33** 2256
[9] Woodruff D P, Hulbert S L, Johnson P D and Smith N V 1985 *Phys. Rev.* B **31** 4046
[10] Altmann W, Dose V and Goldmann A 1986 *Z. Phys.* B **65** 171
[11] Himpsel F J and Ortega J E 1992 *Phys. Rev.* B **46** 9719
[12] Fu C L, Freeman A J and Oguchi T 1985 *Phys. Rev. Lett.* **54** 2700
Richter R, Gay J G and Smith J R 1985 *Phys. Rev. Lett.* **54** 2704
[13] Crampin S 1993 *J. Phys.: Condens. Matter* **5** 4647
[14] Bader S D and Moog E R 1987 *J. Appl. Phys.* **61** 3729
Dürr W, Taborelli M, Paul O, Germar R, Gudat W, Pescia D and Landolt M 1989 *Phys. Rev. Lett.* **62** 206
Himpsel F J 1991 *Phys. Rev.* B **44** 5966
Heinen W, Carbone C, Kachel T and Gudat W 1990 *J. Elec. Spectrosc. Relat. Phenom.* **51** 701
[15] Fedak D G and Gjostein N A 1967 *Surf. Sci.* **8** 77
[16] Wendelken J F and Zehner D M 1978 *Surf. Sci.* **71** 178
[17] Heimann P, Hermanson J, Miosga H and Neddermeyer H 1979 *Phys. Rev. Lett.* **43** 1757
[18] Chiaia G, De Rossi S, Mazzolari L and Ciccacci F 1993 *Phys. Rev.* B **48** 11298
[19] Ciccacci F, Vescovo E, Chiaia G, De Rossi S and Tosca M 1992 *Rev. Sci. Instrum.* **63** 3333
[20] Finazzi M, Bastianon A, Chiaia G and Ciccacci F 1993 *Meas. Sci. Technol.* **4** 234
[21] Samson J A R 1967 *Techniques of Vacuum Ultraviolet Spectroscopy* (New York: Wiley)
[22] This holds true for inverse photoemission (see [8]), better resolutions can be achieved in two photon photoemission, see
Giesen K, Hage F, Himpsel F J, Reiss H J and Steinmann W 1985 *Phys. Rev. Lett.* **55** 300; 1986 *Phys. Rev.* B **33** 5241
[23] Eckardt H, Fritsche L and Noffke J 1984 *J. Phys. F: Met. Phys.* **14** 97
[24] Reihl B and Nicholls J M 1987 *Z. Phys.* B **67** 221
[25] For an exact determination of the image state binding energy, which is referred to the vacuum level, an exact knowledge of the work function measured in situ would be needed. In fact it is difficult to obtain 1×1 surfaces with a very reproducible work function. Unfortunately, such precise measurements cannot be performed in our apparatus. The decrease of the image state energy when going from the 1×1 to the 5×20 reconstruction is however reproducible and consistent with previous studies, see [11].
[26] Crampin S 1994 *Phys. Rev.* B **49** 14035